Spring 2019

Carbon Fiber Monocoque

Dan Brown
djb142@zips.uakron.edu

Leland Hoffman
lch32@zips.uakron.edu

ASME Report Cover Page & Vehicle Description Form

Human Powered Vehicle Challenge

Competition Location: Pomona, CA

Competition Date: March 15th - March 17th

This required document for all teams is to be incorporated in to your Design Report.

Please Observe Your Due Dates; see the ASME HPVC website and rules for due dates.

Vehicle Description

University name: The University of Akron
Vehicle name: Harambe
Vehicle number: 15
Vehicle configuration:
Upright: _____ Semi-recumbent: X
Prone: _____ Other (specify):_____
Frame material: Carbon Fiber, Paper/Phenolic Honeycomb, Oak, Aluminum
Fairing material(s): Carbon Fiber, Paper/Phenolic Honeycomb
Number of wheels: 3
Vehicle Dimensions (m)
Length: 2.629
Width: 0.559
Height: 0.861
Wheelbase: 1.14
Weight Distribution (kg)
Front: 76.3%
Rear: 23.7%
Total Weight (kg): 22.7
Wheel Size (m)
Front: 0.508
Rear: 0.508
Frontal area (m^2): 0.13785
Steering (Front or Rear): Front
Braking (Front, Rear, or Both): Front
Estimated Coefficient of Drag: 0.223

Vehicle history (e.g., has it competed before? where? when?):

Harambe has not competed yet this year. The 2019 ASME E-Fest West Competition will be its first competition.

The University of Akron Human Powered Vehicle Team
2017-2018 ASME E-Fest West Design Report

Vehicle Name: Harambe
Vehicle Number: 15

The University of Akron
College of Engineering

Team Captains:	Leland Hoffman	lch32@zips.uakron.edu
	Patrick Gaertner	pjg41@zips.uakron.edu
Faculty Advisor:	Dr. Scott Sawyer	ssawyer@uakron.edu
Team Members:	Jordan Boos	Ryan Matejka
	Marlee Reynolds	Daniel Brown
	Caleb Miner	Duncan Hamilton
	Victoria McLaughlin	PJ Kennedy
	Leslie Sawyer	Bailey Conard
	Jami Tatulinski	Christopher Morris
	Mike Uy	Zachary Broadbent

Assembly Drawing

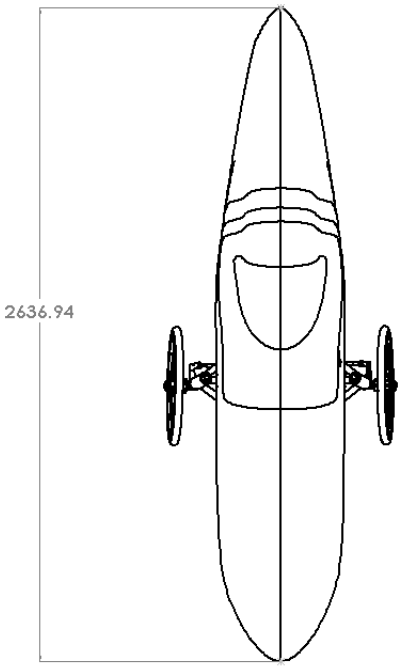

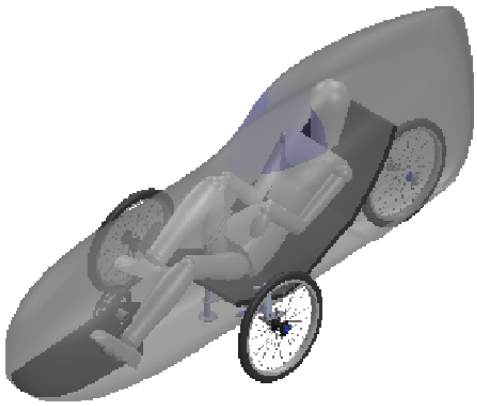

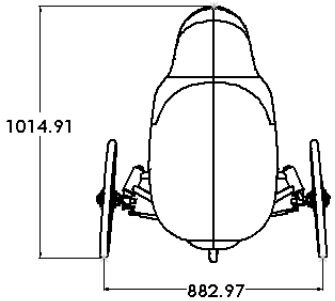

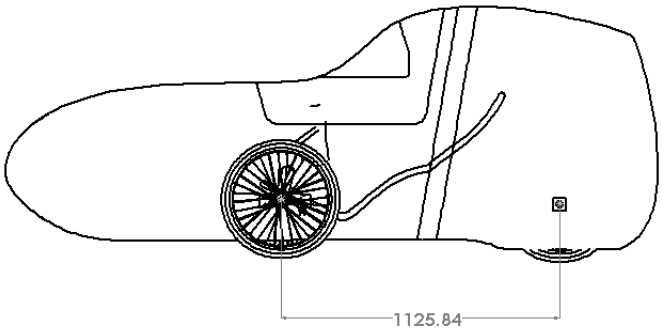

ALL DIMENSIONS IN MILLIMETERS

Abstract

The University of Akron's Human Powered Vehicle Team designed a high performing, fully functioning vehicle that is safe, efficient, and practical for the 2018-2019 season. These objectives were the main priorities when it came to the initial stages of designing the vehicle. In addition, the vehicle was designed in accordance with the ASME 2019 Human Powered Vehicle Challenge guidelines to satisfy all the rules and requirements. Additional priorities have been created to teach practical engineering skills and techniques to the students participating in the project through different points in the production process including research, vehicle design, manufacturing, and testing.

The majority of the work was completed at the University of Akron during the 2018-2019 academic year by undergraduate students from a variety of engineering disciplines. Sub-teams were created to focus on the different regions and systems of the vehicle, including but not limited to, the fairing, steering, suspension, communication, testing, and frame areas. These teams allowed members to take ownership of specific projects and gain in-depth knowledge surrounding their distinct task.

Inspired by UA's Formula Combustion Vehicle, the team is debuting its first monocoque chassis constructed from a carbon fiber/epoxy composite with an aramid honeycomb core. Harambe is a recumbent tadpole trike with all components direct mounted to hardpoints on the chassis. The vehicle will have a fully integrated RPS which will protect against the potential event of an accident or roll-over. Additionally, the vehicle includes a front wheel suspension system, bell crank steering that makes use of a centered steering wheel, contoured seats, and a Bluetooth communication system between the driver and the rest of the team.

Table of Contents

1. Design

1.1. Objective

The University of Akron's Human Powered Vehicle Team designed and manufactured Harambe with the following goals in mind:

- Educate new and returning members in processes of machining and welding
- Improve upon fairing design and manufacturing process
- Maintain or reduce the total vehicle weight
- Improve comfortability of riders with design of a new seat
- Design a communication system that would allow the riders and pits to communicate clearly and effectively during competition
- Ensure compliance with all ASME HPVC rules and specifications

1.2. Background

The popularity of cycling as a method of commuting in urban areas has increased over the past few decades. There has been a 46% increase in cyclist commuters since 2005 [3]. With this influx of cyclists, improvements can be made to increase driver safety as well as efficiency. Improvements include the ability to withstand any incidental impacts from other vehicles and make the vehicle efficient enough so the cyclist can travel to their destination in a timely manner with minimal effort.

While upright, unfaired bicycles are readily accessible and widely used, fully faired models are more efficient. However, the fully faired versions are not as accessible due to the cost of manufacturing. A few additional safety concerns, including a lack of visibility, poor side impact results, and stability also limit the popularity of faired vehicles. These potential limitations were explored during the development of Harambe to develop a solution that would prove effective on a closed course.

1.3. Prior Work

Many of the features that went into Harambe were newly developed this season. From the monocoque chassis to the steering, this year's vehicle has many new features and manufacturing processes that have not been employed in previous seasons.

The Computational Fluid Dynamics (CFD) analysis for Harambe's fairing used the same conditions and procedure as ZC18 in the 2017-2018 season [2].

1.4. Design Specifications

The following criteria for the design and production of the University of Akron's 2018-2019 competition vehicle was derived from the Human Powered Vehicle Competition Rules and Safety Requirements, as well as the design goals set by the team based on previous experiences and current skill sets:

I. The school name or initials must be displayed on the vehicle at least 10 cm high.
II. The vehicle must be able to come to a stop from 25 km/hr in 6 m.
III. The vehicle must be able to start and stop with no outside assistance.
IV. The vehicle must demonstrate stability by traveling in a straight line for 30 m at a speed of 5 to 8 km/hr.
V. The vehicle can have a maximum turning radius of 8 m.
VI. The vehicle must at least have front brakes.
VII. The vehicle must include a Rollover Protection System that prevents the rider from contacting the ground, such that the vehicle should roll over. The RPS should support a top load of 2,670 N at 12 degrees from the vertical, with no visible permanent deformation and a maximum elastic deformation of 5.1 cm. A side load of 1,330 N should also have no visible permanent deformation and a maximum elastic deformation of 3.8 cm.
VIII. The Rollover Protection System must fully and continuously enclose the rider.
IX. Surfaces of the vehicle must be free of sharp edges and hazards.
X. A forward facing field of view at least 180° wide is required.
XI. The vehicle will be designed so that the lowest point is at least 4 in off the ground in order to clear the speed bump during the HPVC endurance challenge.
XII. Design the vehicle with an overall weight of 55 lbs or less so that it can easily accelerate and maneuver at competition.
XIII. Design the vehicle in such a way that it can accommodate and comfortably seat both the tallest and shortest riders on the team.
XIV. Design the vehicle to have a safety factor of at least 2.0.
XV. Design a vehicle that can reach a speed of 40 mph.

1.4.1. Organizational Timeline

In order to have Harambe ready to roll in plenty of time before competition, an organizational timeline was created at the beginning of the designing period to keep the team on schedule.

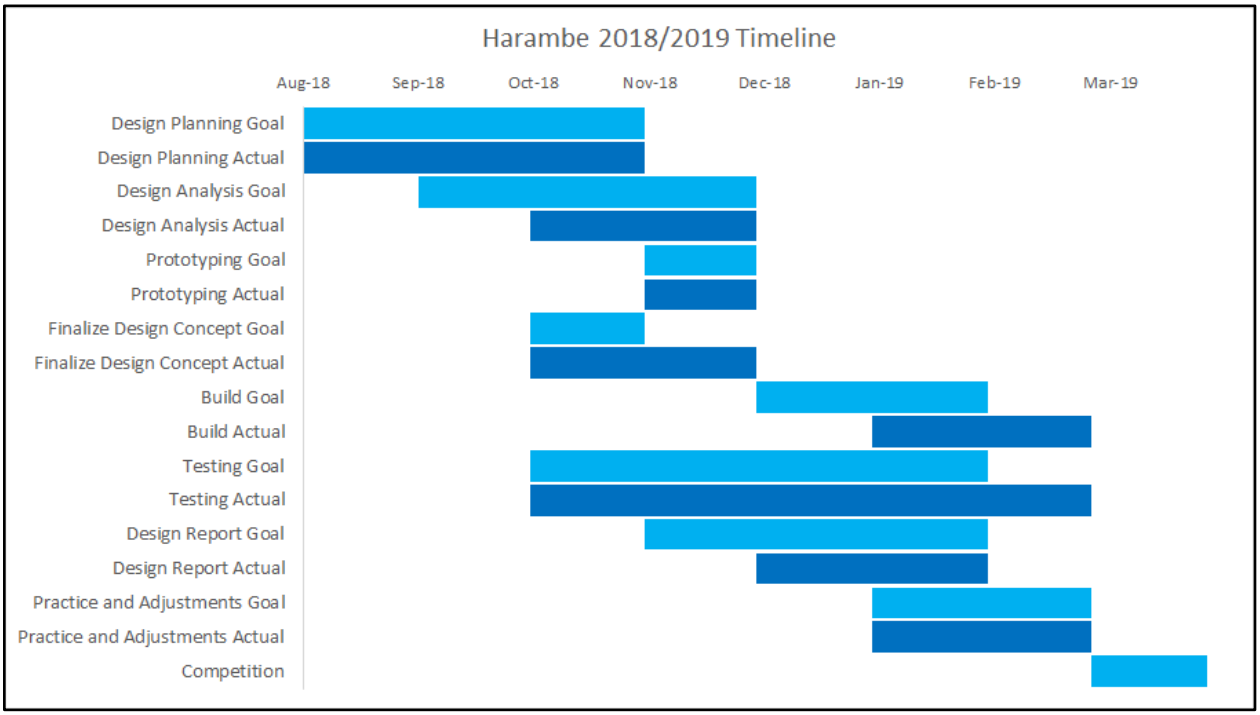

Figure 1: Organizational Timeline

1.5. Concept Development and Selection Methods

The goal of the 2018-2019 season was to develop the best performing vehicle while also adhering to the rules provided by ASME. Each subsection includes a decision matrix weighing the potential choices and how the team selected to components used for Harambe.

1.5.1. Vehicle Style (Refer to Appendix A-1)

The performance of the vehicle, using criteria such as aerodynamics and stability, is largely affected by the vehicle's style. Viable style options included a two-wheel streamliner, delta trike, and tadpole trike.

1.5.2. Fairing Design (Refer to Appendix A-2)

The fairing design was based largely on the results from the power output study (Section 3.1.2.). Aerodynamic capabilities were also a key factor followed by weight and rider comfort. The designs the team faced at the beginning of the year were upright, reclined, and prone positions. Based on these default positions, the fairing would be designed accordingly. After discussion and examination of power output data, the upright position produced the best results.

1.5.3. Fairing Material (Refer to Appendix A-3)

The fairing material chosen for this year was based on a few key factors. Two of the most important factors were weight and stiffness. The team also looked at manufacturability and cost to determine what material would be best for Harambe's fairing. Materials that were considered were carbon fiber, fiberglass, coroplast, and polycarbonate. All of these materials have been used in previous years except fiberglass. Ultimately, carbon fiber was the preferred choice due to its high stiffness to density ratio.

Selecting the core material required the use of CES, a material selection program (Appendix B). A chart of viable materials was created based on compressive strength and density. The primary core should minimize density. It was then obvious that an aramid honeycomb would suffice. Components will be mounted to the chassis using through bolts and will require a material with much higher compressive strength. End grain oak will provide excellent strength and has relatively low density.

1.5.4. Seat Design (Refer to Appendix A-4)

The seat this year was designed in order to be more supportive and better suited to the measurements of each rider. The seat will be constructed of a carbon/honeycomb sandwich. A stiffer material allows the rider to use pressure from the lower back support to drive more power into the pedals. Additionally, by making the measurements more exact to the contours of the rider, the design should be conducive to provide peak performance. Finally, the edges and tight width of the seat will help to hold the rider in an upright position around curves, keeping them secure and centered.

1.5.5. Steering Design (Refer to Appendix A-5)

The final steering design consists of a bell crank system. This style was chosen for multiple reasons. This type of steering can utilize a steering wheel, which is ergonomic and familiar to the riders. Weight was another major factor in this decision. A rack and pinion design was considered; however, It would be considerably heavier and complex to fabricate. The bell crank system is largely made from carbon fiber, reducing overall weight. Wiring for electronics and brakes was internally routed through the shafts of the steering column.

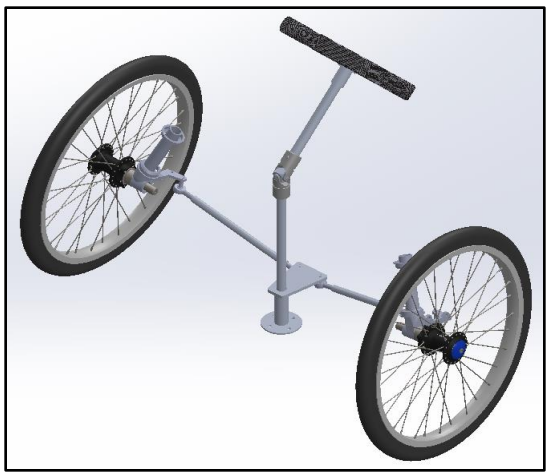

Figure 2: Isometric View of Steering Assembly

1.5.6. Suspension Design (Refer to Appendix A-6)

A partial suspension system was designed to create a smoother ride. Three possible locations were considered for the suspension: the front wheels, the rear wheel, and the seat. Front wheel suspension was chosen for the vehicle based on its ability to provide improved vehicle handling in addition to providing comfort to the rider. From there, four different design concepts were considered: a 4-bar linkage system, a spring damper, an air spring, and a box design, which is common for racing cars. Ultimately, a 4-bar linkage system was chosen for this year's vehicle, as it would be the most adjustable.

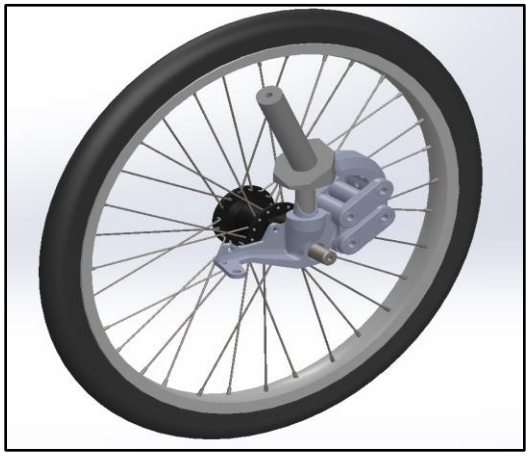

Figure 3: Suspension on Tire

1.5.8. Description of Vehicle

<u>Fairing</u>

Harambe is unlike any of the vehicles the University of Akron has developed in previous years. The reason for this is the structural fairing that completely replaced the aluminum frame used prior. Nomex Honeycomb is the core material used to ensure the strength and rigidity required for a structural fairing. Additionally, the transition toward the honeycomb allows for the vehicle to be more lightweight than in previous years while providing the same, if not more, protection

for the rider. Another new fairing feature this season is the top hatch for rider transition. Previous years' vehicles only had a side-door hatch that was not completely secure or efficient for rider evacuation. Cut into the top hatch is a polycarbonate windshield that contains the only window in the vehicle. While the rider still has 180^{o} of vision required by the rules, minimizing the number of windows ensures the structural integrity and rigidity of the carbon fiber

Component Attachments

Previous vehicles attached the bottom bracket to the frame by means of a 2 inch aluminum tube welded to the frame. This member acted as a cantilever beam in bending and experienced clearly visible deflection under normal loading. In 2018 the team tested this deflection on previous vehicles, Roocycle and Klokan. Klokan had a carbon wrapped tube while Roocycle was left bare. Under maximum pedaling conditions, Klokan deflected 8mm and Roocycle deflected 10mm [2]. This year, with a monocoque chassis, the team developed a mount that was optimized to resist typical pedaling forces. A carbon/honeycomb sandwich panel was chosen, as it provides superior longitudinal rigidity and strength with minimal added weight. Appendix C shows the core layout of the panel. The bottom bracket is bonded inside an end grain oak core. Surrounding the oak is a 38.1 mm honeycomb core. The rest of the panel consists of 19 mm honeycomb core. All bonding will be done using Hysol, a structural adhesive by Loctite that boasts high shear and tensile strengths.

Hardpoints will be bonded in the chassis to allow for direct attachment of the rear wheel. A custom thru-axle will be machined, slide through the hardpoints, and be secured with a quick release.

Seat

This year, the vehicle features two easily interchangeable seats. Using two seat designs allowed for a custom fit for each rider. The seat angle and the back angle were set according to the maximum power output observed in testing (Section 3.1.2). Bolts were used to secure the base of the seat to the fairing. Additionally, the seat was designed with an ergonomic shape to maintain the rider's posture and ensure safety around turns.

It is important to ensure that the seat will not move during races. To eliminate the chance of the seat failing, it was designed to be direct mounted to the fairing with 6 bolts, shown by the black dots in Figure 4. The maximum force in each bolt was calculated by applying the standard 3G vertical acceleration to the mass of the rider and distributing the load evenly between the bolts [1]. The seat was assumed to be a rigid body. It was found that the maximum force on the seat is 2,670 N. Each bolt is required to sustain a shearing force of at least 445 N. Using quarter inch bolts, which have a shear strength of 9,000 N, would give the seat a factor of safety of 20.

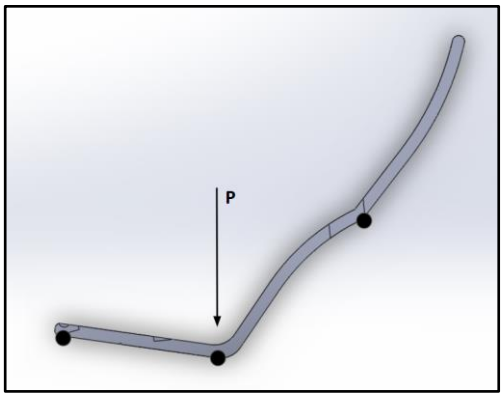

Figure 4: Side view of seat with weight of rider

Communications System

Harambe incorporates a wireless Arduino system for communication between the driver and the pits. It includes LED strips within the steering wheel that change colors based on the message that the members in the pits send to the driver. To respond, there are four buttons signaling different responses, ranging from affirmations to signaling an emergency. Communication to the other drivers on the course is made possible by additional indicators. LED turn signals are activated by pressing left or right on a joystick, brake lights are activated by a limit switch on the brake lever, and a horn to make other drivers aware of Harambe's presence. Lastly, an LCD display was included to print the current lap for the driver as well as the vehicle's speed and the elapsed time (Figure 5). The need for this was developed from rider feedback. One issue was that riders had trouble hearing through a conventional two-way radio while the vehicle was in motion. The decision to use an Arduino system is based upon the availability of parts and their relatively low cost. Additionally, this design allows for further development to the system for future vehicles. These developments can include real-time data acquisition during events to monitor the performance of the vehicle and drivers.

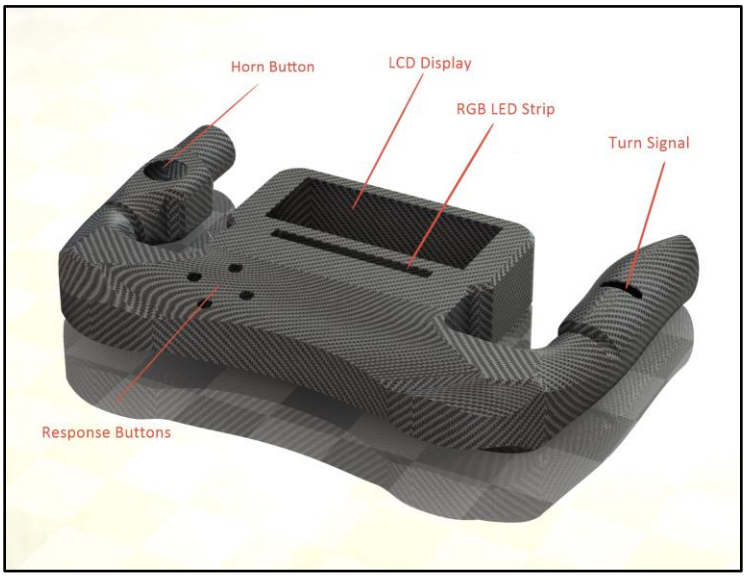

Figure 5: Steering Design

Manufacturing

Having chosen a carbon monocoque chassis, the team needed to perform extensive research and trials. In the past, only non load bearing parts were fabricated. Several techniques were considered as seen in Appendix A-7. In the end, prepreg and lamination were the only methods that would provide a sufficiently strong and lightweight part; however, prepreg was determined to be too expensive. Lamination is a process where carbon is laid over a release film. Next, epoxy is pulled through the fabric using a handheld squeegee. Another layer of release film is laid on top, and the carbon can then be cut to the desired shape using templates.

Another key element to creating a strong and light part is the application of pressure. In the past years, the team used hand layups along with some resin infusion. Both methods used a vacuum bagging setup to apply this pressure; however, a better method is the autoclave. All layups were performed in a sponsor's autoclave, which applied 6.9 kPa to the bagged part. This equates to a force of about 1,200 kN acting downward on each half of the monocoque molds. This will result in much better fiber alignment and allow for lower resin content, which leads to a significantly stronger part.

First, profiles of the model were saved and plotted. These were then traced onto sheets of high density urethane foam and cut out using a bandsaw. Areas of high contour, like the nose, tail, and hatch, required thin sheets while other areas used 3 inch sheets. Each profile had a hole drilled to allow for an aligning dowel. Hysol structural adhesive was applied to both sides of each section and slid onto the dowel. The entire assembly was bagged and put into the autoclave to cure. Foam rasps were used to shape the two halves, and duratec was sprayed on to create a finished surface. A female mold was then pulled from each buck. Finally, the carbon/honeycomb part halves could be laid up. The halves were then bonded on an offset surface using Hysol.

2. Analysis

2.1. RPS Analyses

Table 1: RPS Analysis Summary

Item	Description
Objective	Design a thorough RPS capable of protecting the driver in the event of an accident.
Assumptions	The hatch is considered negligible in this analysis.
Methods	Use Solidworks Simulation to study deformation caused by loading representative of various accident scenarios. Simulate impact by applying force where contact will occur.
Results	The maximum deflection in the top load case was 1.01 mm. The maximum deflection in the side load case was 10.96 mm.

2.1.1. Methods

In any engineering application, safety is a priority. Implementation and analysis of the RPS is essential to certifying the safety of the rider. Two worst case scenarios were considered during the analysis. The top loading case involved applying a force of 2,670 N (600 lbf) downwards and towards the rear of the vehicle, 12 degrees from the vertical. This force is suggested to be an approximation of the force seen in the event of a vehicle rollover. The side loading case required the application of a 1,330 N (300 lbf) force applied horizontally to the side of the vehicle at approximate rider shoulder height and location. Guidelines depicting a secure vehicle subjected to the conditions explained were outlined in the rules.

Solidworks Simulation was used to analyze the RPS. The monocoque was modeled as a surface and meshed with shell elements. Three shell element compositions were developed and assigned based on the three types of sandwich configurations used in the monocoque. Custom materials were created to verify that materials modeled into Solidworks had the same characteristics as those used in construction. Material properties were found using CES software along with testing data from previous years [2].

2.1.2. Results and Conclusions

The top load of 2,670 N force was applied directly above the riders head. The force was reacted by the harness attachment points. Maximum deflection of the integrated RPS was 1.01 mm. This result was well within the elastic deformation criteria of maximum 5.1 cm. Results of the loading analysis can be seen in Figure 6.

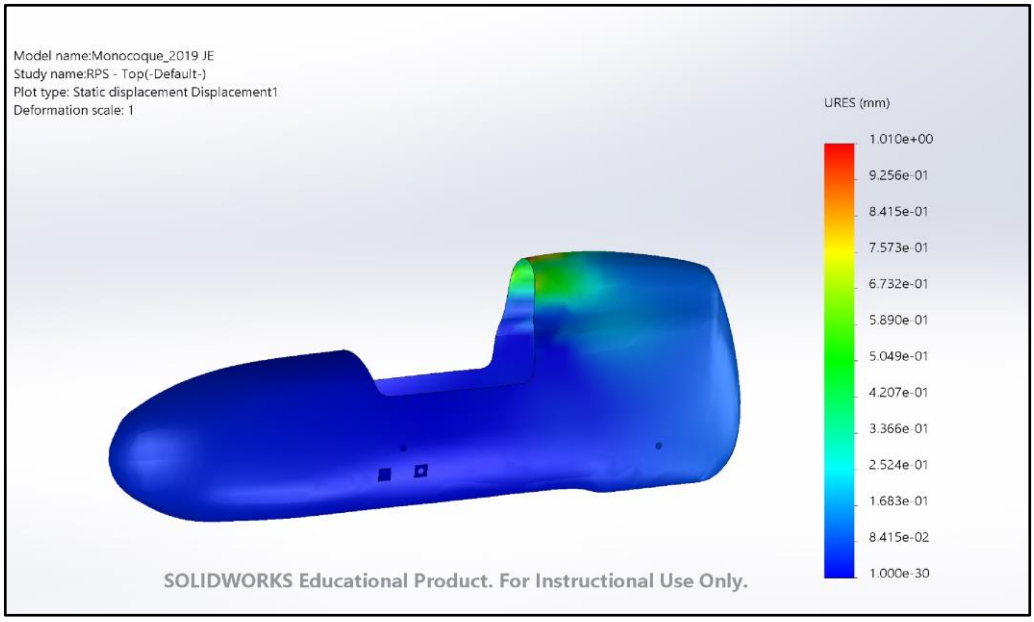

Figure 6: RPS FEA Top Load Condition

The side load of 1,330 N force was applied horizontally to the integrated RPS at rider shoulder height. Again, this force was reacted by the harness attachment points. Results seen in Figure 7

show the maximum deflection to be 10.96 mm. This greatly exceeds the requirement of 3.8 cm maximum elastic deformation.

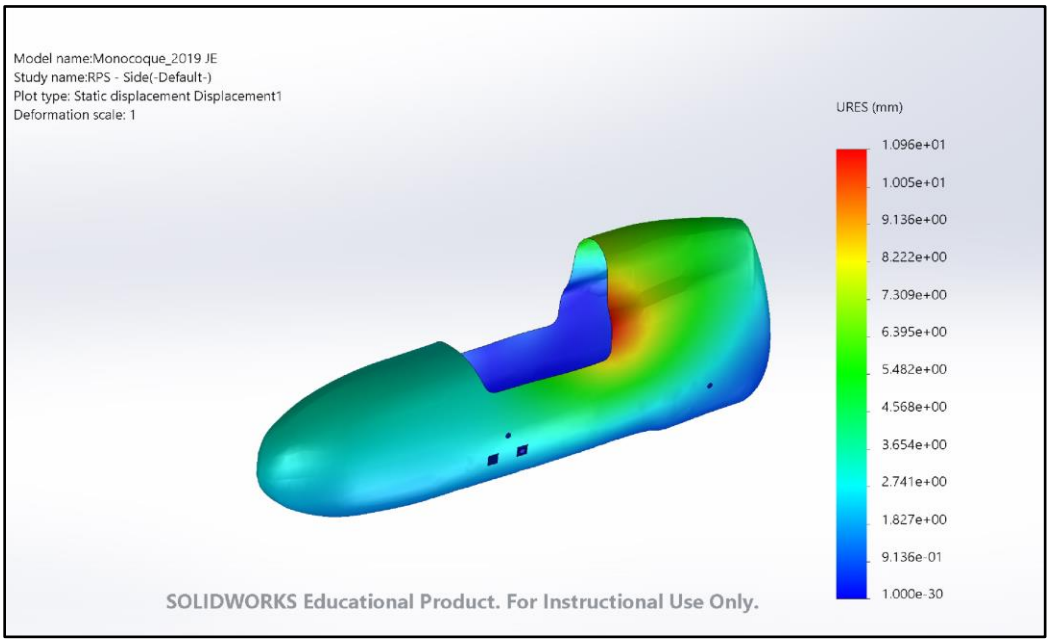

Figure 7: RPS FEA Side Load Condition

As shown in Figures 6 and 7, the load experienced by the vehicle can sufficiently be absorbed and dissipated by the RPS. The load travels from its point of contact and is split by the symmetric ends of the RPS hoop. The harness is more than capable of supporting and restraining the rider in these instances.

From rider to ground, the load path can be visualized starting at the harness points. For the top load case, the vehicle is simulated rolling over and is inverted. The load path moves from the lower harness points by the rider's hips to the upper harness points by the rider's shoulders. Then, the load path moves up the RPS and around the fairing to meet at the point where the load is applied. From here, the load is transferred into the ground. Figure 8 demonstrates this load path on one side of the vehicle. Both sides of the vehicle have identical load paths.

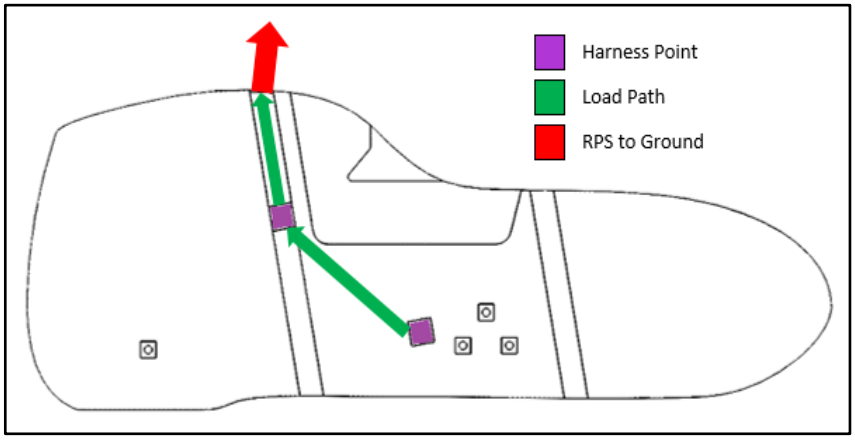

Figure 8: Top Load Path Scenario

In the side load case, the load paths also originate at the harness points. The harness points near the rider's hips travel towards the rear of the vehicle until meeting the RPS. The load path from the ground-side hip harness point can then travel directly into the ground. The load path on the opposite side must first travel through the harness point by the rider's shoulder opposite of the load. This path then travels up and across the RPS before transferring to the ground. This case can be seen in Figure 9.

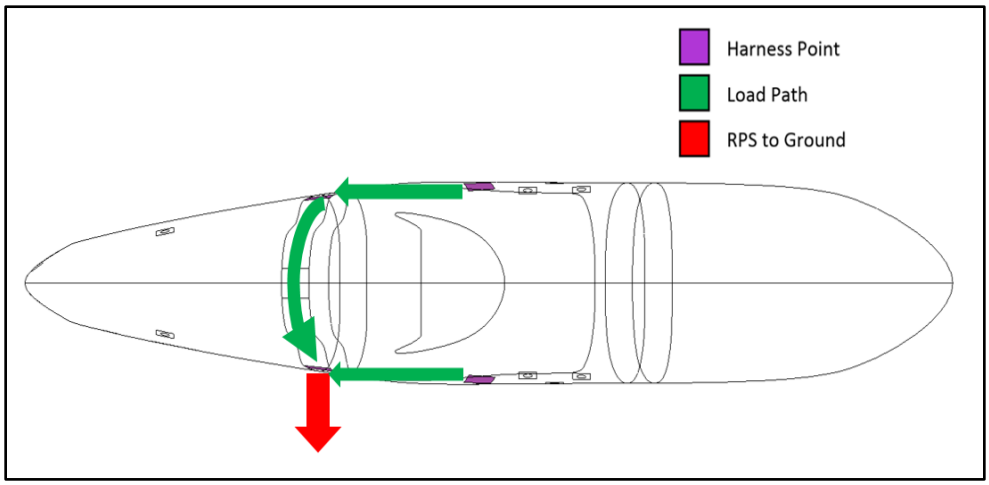

Figure 9: Side Load Path Scenarios

2.2. Structural Analyses

Table 2: Structural Analysis Summary

Item	Description
Objective	Design a vehicle to support loading scenarios experienced during competition.
Assumptions	Assume average rider weight for both speed bump and breaking scenarios. Von Mises failure criterion for ductile materials.
Methods	Use Solidworks Simulation to analyze deformation caused by various loading scenarios.
Results	Maximum deformation of 0.352 and minimum factor of safety of 2.12.

2.2.1. Methods

Using Solidworks Simulation, the head tubes were analyzed for the case of the vehicle encountering a speed bump. The head tubes will be welded to an aluminum plate that is then bolted through the end grain oak core in the fairing. The faces that will be welded to the plate are assumed to be fixed. When traveling over a speed bump, the vehicle is assumed to experience 3G forces, and with the average rider's weight, a reaction load of 2669 N (600 lbf) was calculated. This load was vertically applied to the head tube for the simulation.

The head tubes were also analyzed for the braking scenario. As described in section 3.1.2., a test was designed to calculate the forces on the vehicle caused by braking as hard as possible without the vehicle skidding, or the rear wheel lifting off of the ground. This force was determined to be

approximately 870 N (195.6 lbf). Based on previous experience, the head tubes were determined to be sufficiently strong enough, that the force was applied to the outside of the tube.

Next, the bottom bracket panel, or BB panel, was analyzed. Given a typical maximum pedaling force of 1400 N [1] and a crank length of 175mm, a 250 Nm torque was applied to the panel at the location where the bottom bracket will be bonded. The bottom bracket itself was assumed to be sufficiently strong based on its usage on previous vehicles and was omitted. The panel was bonded to the chassis and the torque was reacted at the seat mount points.

2.2.2. Results and Conclusions

In the speed bump scenario analysis, shown in Figure 10, an element size of 5.12 mm was used. The head tube deformed a maximum of 0.26 mm on the edge of the tube opposite of the mounts and the load that was applied, and the minimum factor of safety was 2.89. This exceeds the design goal set of a minimum factor of safety of 2.0. It should be noted that this loading scenario was only applied to one head tube, where in competition, the load would be distributed to both head tubes relatively evenly. This increases the level of confidence placed on the head tubes to not deform under the speed bump scenario.

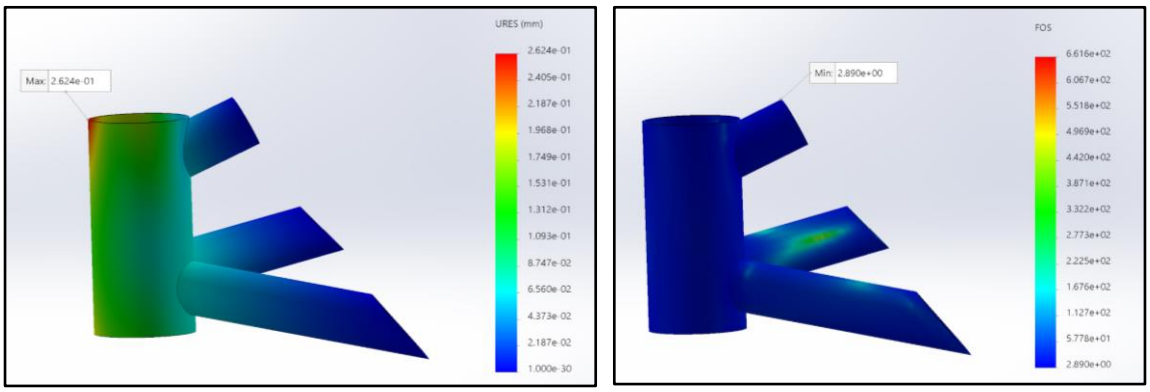

Figure 10: a) Displacement and b) Factor of Safety

When the head tubes were analyzed for the break force scenario, the maximum deformation was 0.352 mm and the minimum factor of safety was 2.12. Like with the speed bump scenario, the element size remained at 5.12 mm. This is shown in Figure 11. Again, this analysis applied the full force to only one head tube, where in reality, the force would be distributed between each head tube on either side of the vehicle.

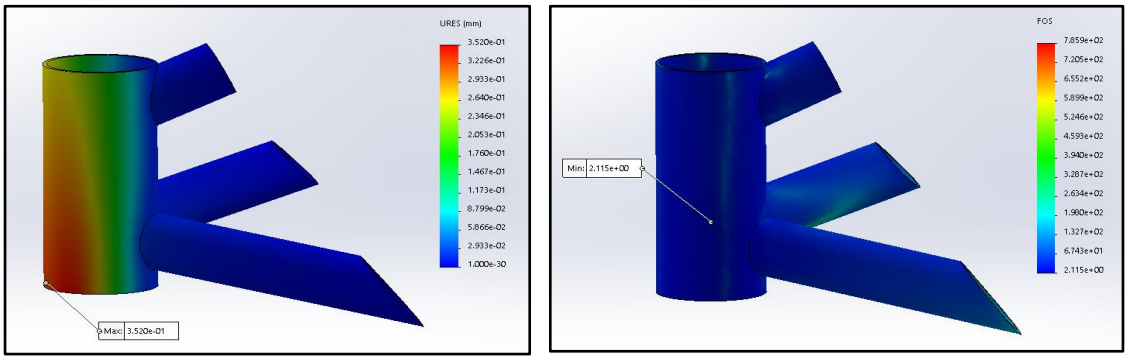

Figure 11: a) Displacement and b) Factor of Safety

As seen in Figure 12, the BB panel will see only 0.28 mm deflection. The only area of concern is the stress concentration located around the BB mount visible in Figure 13. This is likely due to the step down in core size at that location. In order to help evenly distribute the load into the rest of the panel, each core will be chamfered to create a more gradual step down to the next core thickness.

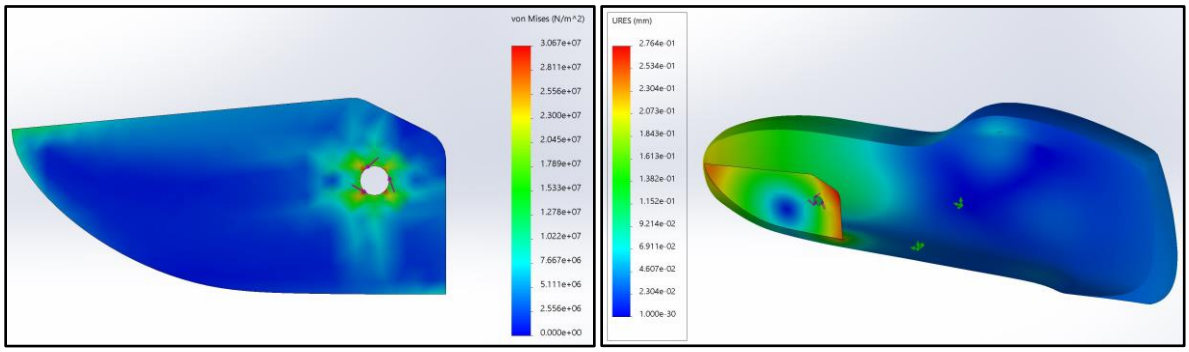

Figure 12 and 13: Structural Analysis of BB Panel

2.3. Aerodynamic Analyses

Table 3: Aerodynamic Analysis Summary

Item	Description
Objective	Design a fairing with a minimal drag force and drag coefficient.
Assumptions	The wheels have a negligible effect, as well as the rivets securing the windows and hatch. Conditions are at sea level.
Methods	Use SolidWorks Flow Simulation to analyze the aerodynamics of the proposed fairing design.
Results	Maximum drag force of chosen design is 6.15 N and maximum drag coefficient is 0.25.

2.3.1. Methods

Using Solidworks Flow Simulation, airflow was simulated at various velocities to mimic riding conditions and predict the subsequent drag force on multiple iterations of fairing design. Three iterations were analyzed before deciding on the final design and are shown in Table 4. During the drag race, the vehicle can reach speeds of approximately 40 miles per hour. Tests were performed from 10 mph to 40 mph in increments of ten in order to get the best approximation of the drag coefficient. Additionally, one test was run with a longitudinal velocity of 40 mph, with a 10 mph crosswind added in the transverse direction. This was done to prove that any crosswind would not threaten the stability of the vehicle during the course of the competition.

Table 4: Revisions of Fairing Design Analyzed

Revision 1	Revision 2	Revision 3
		

In addition, an analysis was performed to evaluate the addition of air ducts to the final fairing design. In previous years, riders have suffered from heat fatigue while riding in fully enclosed vehicles. A typical remedy during the endurance portion was to omit the hatch, allowing enough airflow to cool the rider. However, this was not without a severe aerodynamic penalty. The open hatch with no outlet acts like a small parachute. The team has elected to incorporate a cooling system in the form of strategically placed NACA ducts. Unlike the protruding scoop style vents, NACA ducts aim to draw in air while avoiding the addition of form drag and separation of the flow. One inlet duct and two symmetrical outlets can be seen in Appendix D-1.

2.3.2. Results and Conclusions

For each vehicle revision, when the 10 mph crosswind was added to the case of the vehicle traveling at 40 mph, a large force acted on the vehicle in the transverse direction. This force was, at minimum, five times that of the longitudinal force for each fairing iteration. Table 5 depicts the force in the direction of the crosswind for each of the revisions. While Revision 2 had superior drag coefficients across the board, it was affected more than the other two in terms of a crosswind. This is due to Revision 2's large side area. In the case that there would be any type of cross wind during competition, the team determined that Revision 2 should not be utilized.

Table 5: Force on Each Fairing Revision Caused by the Crosswind

Fairing Revision	Force Perpendicular to Vehicle (N)
1	50.469
2	67.174
3	53.410

The results for drag coefficient for each revision at each of the speeds analyzed is shown graphically in Figure 14. While comparing Revision 1 and 3 for the final design, it is evident that the drag coefficient values are within a relatively small range of for each speed. Choosing to use Revision 3, the highest speed of 40 mph created a drag force of 6.146 N (1.382 lbf) and had a drag coefficient of 0.228. Table 6 details the drag forces and drag coefficients for Revision 3. The pressure distribution for the 40 mph speed and the 40 mph speed with a 10 mph crosswind for Revision 3 can also be seen in Figures 15 and 16,0 respectively.

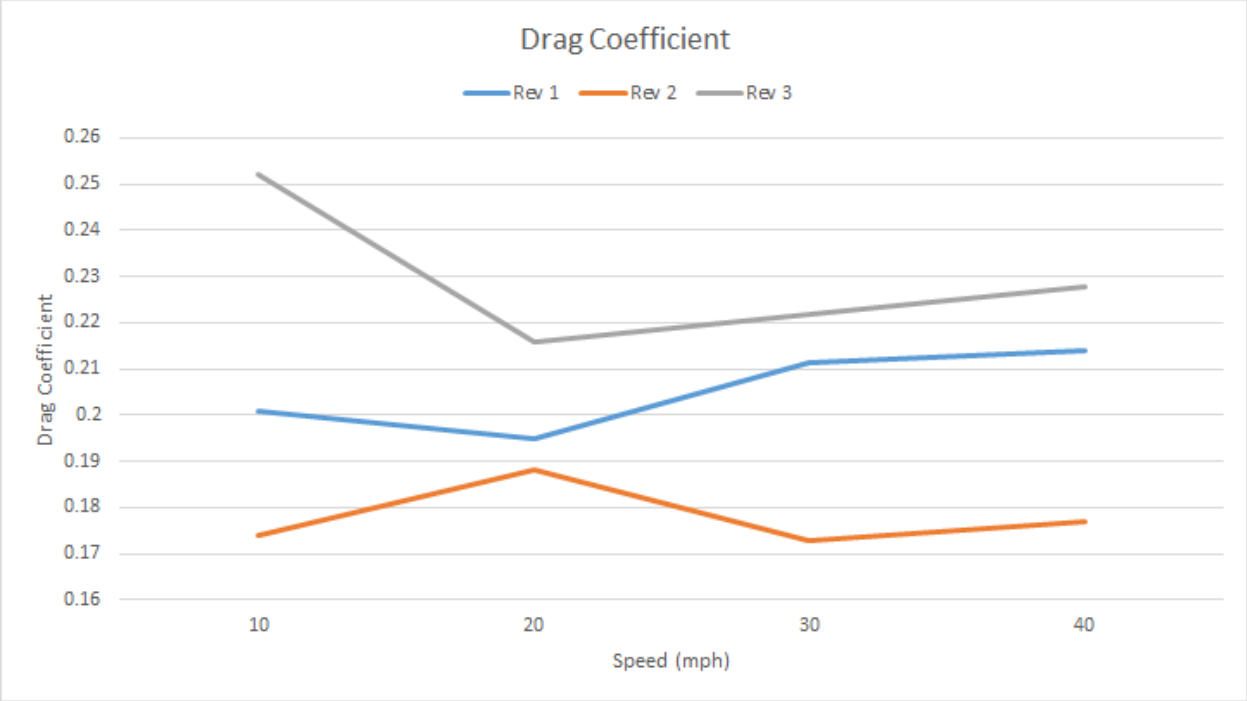

Figure 14: Drag Coefficients of Fairing Revisions

Table 6: Effects of Velocity on Drag

Speed	Drag Force (N)	C_D	C_DA (m^2)
10 mph	0.425	0.252	0.034
20 mph	1.458	0.216	0.030
30 mph	3.371	0.222	0.031
40 mph	6.146	0.228	0.031

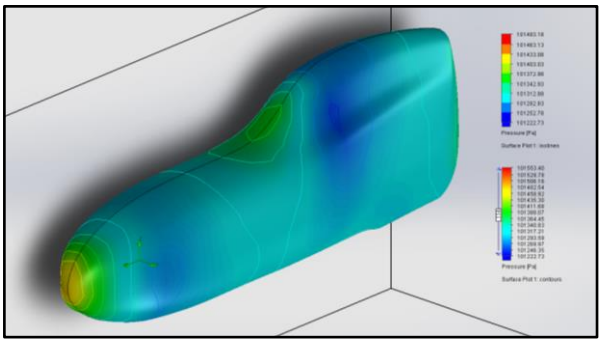

Figure 15: Pressure Distribution at 40 mph

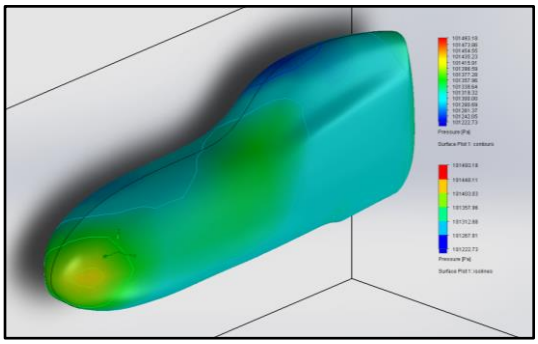

Figure 16: Pressure Distribution at 40 mph with 10 mph crosswind

The drag force and drag coefficient were extremely important considerations for designing the fairing. In addition to analyzing aerodynamics, the team also took into account the best shape for making the fairing structural. This is why Revision 3 was chosen over Revision 1. In order to incorporate the proper field of vision in accordance with the rules, Revision 1 would require a large area of the fairing to be cut out to allow for windows. This is not ideal for a structural fairing because the removal of too much carbon fiber in any area can compromise the strength of the fairing. Revision 3 only needs a polycarbonate windshield to allow for full vision, therefore minimizing the removal of material.

The aerodynamic analysis performed for the air ducts determined if the ducts would effectively route air past the riders head and out the rear. Using the same method described for the analysis of the various fairing revisions, a longitudinal velocity of 20 mph was applied and the drag force and $\boldsymbol{C_D}$ were determined to be 1.486 N and 0.220, respectively. The slight increase in drag was determined to be a worthwhile investment. Flow trajectory through the duct can be seen in Appendix D-2.

2.4. Cost Analyses

At the beginning of the design cycle, the University of Akron's Human Powered Vehicle Team set out to design Harambe as a monocoque trike, eliminating the need to have a vehicle frame. This however meant that more funds had to be allocated to the fairing and more extensive research needed to be done on materials in order to make the fairing more structurally stable. The team however wanted to keep costs of the entire vehicle to no more than $6,000, which is similar to the total cost of ZC18.

By removing the cost of fabricating a vehicle frame for this year, the team was able to allocate additional funds to creating a new suspension and steering system in addition to the additional fairing funds required. This new suspension system will allow for a smoother ride during the endurance race, and the new steering system will allow the new communication system to be more easily implemented as well as give the rider a central point to both receive and send communications from and to the pits.

The total cost to produce the vehicle for this year is shown in Table 7 below and totals to $5,487.97 with the budget for the year being $6,000.00. The cost of Harambe is broken down to include purchased components, materials, labor, and tools as well as full costs of donations that were made to the team from sponsors.

Table 7: Cost Analysis Chart

Product/Labor	Cost
Components	$2,346.61
Fairing mold material	$1,000.00
Fairing raw material	$1,050.13
Fairing reinforcing material	$449.90
Tools	$191.33
Steering	$100.00
Suspension	$200.00
Communication	$150.00
Total	**$5,487.97**

As expected, the majority of costs for Harambe came from components and fairing, which the team has experienced before. The difference with Harambe was that fairing materials cost about $153.42 more than components. The fairing of Harambe costs about 18.3% more compared to ZC18, and accounts for nearly 45.6% of the total costs of Harambe as shown in Table 8.

Table 8: Percentages of total budget

Category	Percentage of budget spent
Fairing	45.6%
Components	42.8%
Tooling	3.49%
Suspension	3.64%
Communication	2.73%
Steering	1.82%

2.5. Other Analyses

2.5.1. Suspension Kinematics and Dynamics Analysis

Table 9: Suspension Kinematics and Dynamics Summary

Item	Description
Objective	Determine ideal stiffness of elastomers used for front wheel suspension.
Assumptions	Rider weight, maximum impulsive force exerted on the wheels, and maximum elastomer deformation are approximated and constant.
Methods	Calculate theoretical approximation of required stiffness constant using Hooke's Law.
Results	Ideal elastomer stiffness is calculated to be approximately 2.2×10^4 N/m.

A front wheel suspension system on a semi-recumbent tricycle reduced the vibrations experienced by the rider due to normal operation, and over uneven terrain. This resulted in improved handling of the vehicle, as well as a more comfortable ride. In order to design a suspension system that would have optimal performance capabilities, calculations were performed using approximations of the average rider weight, impulsive forces exerted on the vehicle at top speeds, and the maximum range of motion for the suspension system. This was done to determine the ideal stiffness constant for the necessary elastomers.

Hooke's Law was used to give an approximation of the necessary stiffness constant through the equation: $F = kx$. Here, x is the range of motion that is desired for the suspension, F is the net force exerted on each wheel, and k is the stiffness constant of the elastomer used for the suspension system. As stated in the structural analysis, the total 3G force exerted on the wheels by a rider of average weight going over a speed bump was determined to be 2,669 N. Taking 30% of this value gives the approximate force experienced by a single wheel. Thus, for a desired range of motion of 40 mm for the suspension system, it was calculated that an ideal elastomer will have a stiffness constant of 2.2×10^4 N/m.

2.5.2. Ackerman's Analysis

Table 10: Ackerman's Analysis Summary

Item	Description
Objective	Determine range of turn angles that achieve most efficient steering.
Assumptions	Rigid body. Wheels roll without slip. Vehicle is moving at low speeds.
Methods	Matlab program and calculations.
Results	Steering geometry to achieve required steer angles.

The main use of Ackerman's fundamental equations of steering geometry for Harambe was to analyze the independent steer angles required to achieve efficient steering. A MATLAB program (Appendix E) was developed to produce a range of angles (inner and outer) that would be suitable for a range of turn angles. It should be noted that according to *Design of Human-Powered Vehicles* by Mark Archibald, the angles calculated using Ackerman steering formulas are exact for only two angles: one for neutral steer and for a small turn angle. From the developed angles, it can be seen in Figure 17 that the inner and outer steer angles deviate most at large turn angles, which are required for small track radii. Ackerman's compensation was used as a way for the steering geometry to be validated in the sense that the geometry appears to achieve the required steer angles. Up to about 15° inner tire turn angle, the steering satisfies the Ackerman steering angle. This was expected though as Archibald's book states that the steering mechanism used is incapable of attaining the Ackerman angles exactly. An attempt was made by the team to minimize the steering error. To accomplish this, the lengths of the tie rods were decreased. Also, the length of the bell crank had to be altered so that its length is similar to the length of the steering arm on the spindle assembly [1].

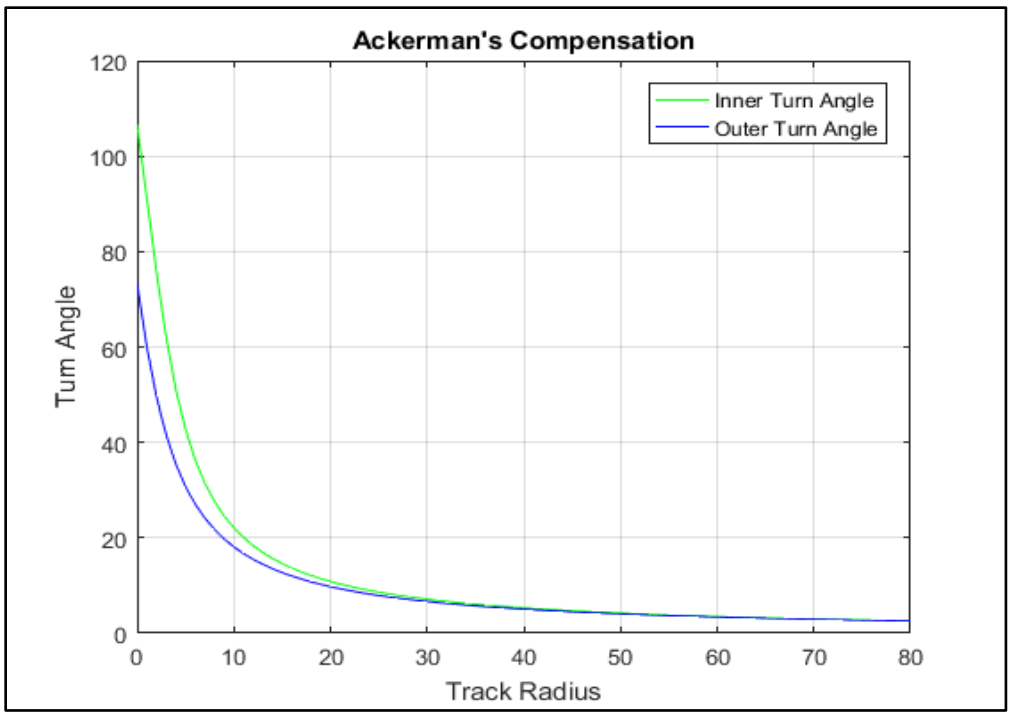

Figure 17: Turn Angle (degrees) vs Track Radius (in)

2.5.3. Drivetrain Gearing Analysis

Table 11: Drivetrain Gearing Analysis Summary

Item	Description
Objective	Determine optimal gearing ratio for best performance.
Assumptions	No change in cadence for each study.
Methods	Calculating speed and power.
Results	Drivetrain was optimized using the results of these studies.

Given the choice of a 20 inch rear wheel diameter, a large 68 tooth chainring was chosen. This was so no intermediate gears were necessary to achieve 40+ mph top speed in the drag event, and an off-the-shelf cassette and derailleur could be used. The gear range was selected to be able to perform at high speeds for drag racing, as well as have low gearing for climbing potential hills at a reasonable pedal cadence and power output in the endurance race. A 10-speed cassette was chosen because 10-speed chain can be bought by the foot, eliminating the need to link multiple chains together, thus reducing the chance of a chain break.

For speed and power output, three pedal cadences were used: 55 rpm to simulate a rider struggling up a hill, 80 rpm to simulate a good cruising cadence, and 100 rpm to simulate sprinting. To ensure sufficiently low gearing, a grade of 10% was used in the calculation for power required for climbing a hill. The 10 tooth cog is the smallest cog on a standard bicycle cassette, the largest cog size was increased in size until speed and necessary power output were low enough to be achievable by all riders when climbing a 10% grade at a 55 rpm pedal cadence.

Speed was calculated with Equation 1 using pedal cadence, number of chainring teeth, number of cassette teeth, and wheel circumference.

$$v = N_{cadence} \frac{N_{chainring}}{N_{cassette}} c_{wheel} \quad (1)$$

Power was calculated with the Equation 2 using total mass of the vehicle and rider, acceleration due to gravity, hill grade, and speed.

$$P = m_{total} g \cdot grade \cdot v \quad (2)$$

Table 12: Results of calculation for speed and power

Cadence (rpm)	Cassette teeth	Speed (mph)	Climbing Power Output (Watts)
55	10	23	N/A
80	10	34	N/A
100	10	42	N/A
55	36	6.5	260
80	36	9.4	375
100	36	12	470

3. Testing

3.1. Developmental Testing

3.1.1. Development of Designs from Rider Dimensions

Table 13: Development of Designs from Rider Dimensions Summary

Item	Description
Objective	Design an ergonomic vehicle.
Assumptions	Measurements are taken to consistent points on each potential rider.
Methods	Take rider measurements to design the vehicle around.
Results	Seat and steering systems designed to be ergonomic for all riders.

An ergonomic design is essential for each rider to be able to perform their best, and comply with all safety regulations. Looking at the main riders selected for the 2019 competitions, there was a large variety in shape and size. The tallest rider needed sit in the vehicle and have the RPS still properly protect his head, and the shortest rider needed to be able to reach the pedals without slouching down in the seat and compromising visibility. With the team implementing a new steering design in the vehicle this year as well, each rider would need to be able to reach the wheel comfortably.

Key body dimensions were taken for each member of the team at the beginning of the year. This was used to develop a rider volume to simulate a rider pedaling the vehicle while designing it. When riders were chosen for competition, their measurements were averaged and analyzed. The summary of measurements can be seen in Table 14, while the table containing details on riders' individual measurements can be seen in Appendix F. The measurements specifically for riders were used in designing the seats for Harambe. Measurements for the upper leg, lower back, and torso length were key to fitting the seat model to the specified group of riders. Leg length and torso length were used in developing the steering system as well.

Table 14: Rider Dimension Summary

Measurement	Average	95% Confidence Maximum	95% Confidence Minimum
Total Height (in)	68.90	72.04	65.76
Leg length (in)	36.95	39.75	34.11
Top of Knee to Bottom of Foot (in)	21.75	23.48	20.02
Torso Length (in)	23.95	25.46	22.44
Lower Back Length (in)	9.10	10.60	7.60
X-Seam (in)	41.95	43.83	40.07
Heel to Toe Length (in)	9.55	10.10	9.01
Shoulder Width (in)	18.15	18.95	17.35
Shoulder Width (in)	7.20	7.77	6.63
Hip Width (in)	14.75	15.48	14.02
Arm Length (in)	30.35	32.00	28.70

3.1.2. Rider Configuration

Table 15: Rider Configuration Test Summary

Item	Description
Objective	Determine ideal back, hip orientation, and body configuration angles for seat design.
Assumptions	A steady heart rate can be maintained by each rider.
Methods	Perform power output tests using an adjustable weight bench for three riders.
Results	The seat will be designed with back, hip orientation, and body configuration angles of 42°, 8°, and 130° respectively.

Three athletes performed six tests of various back, hip orientation, and body configuration angles, as defined in the table in Appendix G-1 [1]. The back angle, BA, is defined as the angle

between the horizontal and the back of the rider. The hip orientation angle, HOA, is the angle from the hip joint center to the horizontal. Lastly, the body configuration angle, BCA, is that from the torso to the line that defines the hip orientation angle. These angles are demonstrated in Appendix G-2. The athletes performing these tests were given a heart rate monitor and instructed to maintain a consistent heart rate while pedaling on the testing setup. Keeping a constant heart rate, plus or minus approximately 5 beats per minute, their power output was recorded and then compared from configuration to configuration, as seen in Appendix G-3.

Originally, the BCA was thought to be the main factor driving the amount of power that could be produced by an athlete. Tests one and six were designed to evaluate this theory, having the same BCA, and varying HOA and BA. Analyzing the results for these two configurations proved that this assumption was not entirely accurate. Test one showed that a large HOA and smaller BA gave very low performance ratings. Test six implemented a small HOA and a large BA, and provided a much better performance. While the BCA is still important, the conclusion was made that power output depends more on a delicate balance between both BCA and HOA than on BCA alone.

Creating a scatter plot with data points marking heart rate versus power output showed that many of the angle combinations were competitive with each other. These results can be seen in Appendix G-4, which represents the average outputs for all of the athletes that participated in this test. Only one test stood out as producing a lower power output at a heart rate consistent with the rest of the tests. This was test one, which had the highest HOA. Mark Archibald writes in *Design of Human-Powered Vehicles* that higher HOAs tend to produce less power, which was proven in this test's results. While most of the other results were fairly consistent with each other, test three was chosen as the configuration to be used for the frame design. In viewing the results, this configuration of angles was either on par or above average for each of the athletes in terms of power output compared to heart rate. This configuration also had a relatively larger BCA compared to some of the other tests, which Archibald said creates an advantage in the amount of power that the rider can theoretically produce over longer rides. While this test was performed over a much shorter period of time, the benefits of this will be seen in the endurance race at competition, where each rider is typically in the vehicle for 30 to 40 minutes [1].

3.1.3. Brake Force Testing

Table 16: Brake Force Testing Summary

Item	Description
Objective	Determine the force acting on the vehicle while breaking to use for analysis.
Assumptions	No skid.
Methods	Use a vehicle from a previous year to acquire the data needed to evaluate the force.
Results	Brakes have a maximum brake force of 873.21 N.

This test was conducted on damp pavement to mimic the worst case environment. To calculate a maximum force, the rider traveled at a steady speed of approximately 6 m/s, then hit the brakes at a designated stopping point. The distance it took the vehicle to reach complete stop was recorded. This process was repeated 15 times. Average acceleration was calculated for each trial

using the kinematic equation, $V_f{}^2 = V_i{}^2 + 2ad$. V_f represented final velocity, V_i represented the initial velocity, a represented acceleration, and d represented the distance required to stop.

Next, the force of brakes was calculated by taking the acceleration and multiplying it by the mass of the vehicle and rider.

To verify that the break force would suffice, the pitch over limit was estimated using equations found in Mark Archibald's *Design of Human-Powered Vehicles*. To find the pitch over limit, first the center of mass to rear axle, center of mass to ground, and wheelbase lengths had to be found. Next these values were plugged into Equation 3 to find pitchover limit [1]:

$$A_{pitchover} = \frac{L-b}{h} \qquad (3)$$

$A_{pitchover}$ = pitchover limit

L = wheelbase

b = center of mass to rear axle

h = center of mass to ground

Using values of 0.870 m, 1.140 m, and 0.412 m for b, L, and h respectively, the pitchover limit was found to be 0.6545, this value is unitless due to the in/in units after calculation. The pitchover limit was then multiplied by the weight of vehicle plus a 717.72 N rider to find the break force, which came out to be a value of 575.82 N. This calculated value is 297.39 N less than the break force value found through testing. This proved that Harambe's braking system more than satisfies the minimum required braking force found using the pitchover limit.

4. Conclusion

4.1. Comparison

Table 17: Comparison of Design Goals, Analysis, and Testing

Parameter/Objective	Outcome
Design the vehicle in such a way that it can accommodate and comfortably seat both the tallest and shortest riders on the team.	Rider dimensions were taken and used for the steering system and a new seat design were created to ergonomically fit all riders.
Design the vehicle with an overall weight of 55 lbs.	Harambe's total weight was projected to be approximately 50 lbs or 22.7 kg.
Design the vehicle to have a safety factor of at least 2.0.	Structural analysis shows that Harambe's design ensures a minimum safety factor of 2.89.
The vehicle can have a maximum turning radius of 8 m.	To be tested and shown in the performance video.
The vehicle must comply with all ASME HPVC rollover system specifications.	Finite Element Analysis shows that Harambe will comply with ASME specifications.
Improve upon fairing design and manufacturing process.	Harambe's fairing decreased its frontal area by 0.371m when compared to ZC18, and manufactured a female mold from a male mold to yield a better more accurate finish on the final product.

4.2. Evaluation

The University of Akron Human Powered Vehicle underwent significant changes for the 2019 season. Many hours of research and analysis led to a vehicle that is both visually and functionally different than in previous years. These changes are meant to enhance the lightweight capabilities of the vehicle while also improving on safety and performance. Despite these changes, all requirements and specifications set forth by ASME were met and verified through simulation and testing. The most important change of this year being the structural fairing that replaced previous years' aluminum frame as the RPS. This eliminated welding and heat treating, minimizing lost time where the vehicle was not in the shop. Other changes/improvements focused on the drive train with an upgraded steering system and suspension package. This goal focuses on improving rider performance and comfortability for competition. All objectives and specifications of the 2019 vehicle were satisfied.

4.3. Recommendations

From a frame and steering standpoint, a larger emphasis should be placed on Ackerman's Compensation and should be further researched in the future. The current program should be optimized and expanded upon pending research. The data from the new calculations should play a larger role in dictating steering and frame geometry.

The fabrication process of the monocoque molds was very labor intensive and tedious. In the future, these molds should be CNC machined to reduce workload and improve accuracy.

5. References

[1] Archibald, Mark. *Design of Human-Powered Vehicles*. The American Society of Mechanical Engineers, 2016.

[2] The University of Akron Human Powered Vehicle Team, “2018 HPVT Design Report - East - ZC18,” Akron, Ohio, 2019.

[3] The League of American Bicyclists. “Where We Ride: Analysis of Bicycle Commuting in American Cities.” 2016. PDF file.

[4] Ashby, Michael F. *Materials Selection in Mechanical Design*, 5th Edition, Elsevier, 2018.

6. Appendices

Appendix A: Design Matrices

Appendix A-1: Vehicle Style Decision Matrix

Parameters	Weight	Tadpole Trike	Delta Trike	Streamliner	Quad
Performance	20%	4	4	4	2
Aerodynamics	20%	3	4	5	2
Weight	25%	3	3	4	2
Stability	25%	4	3	1	5
Past Experience	10%	5	3	1	1
Total	100%	3.65	3.4	3.15	2.65

Appendix A-2: Fairing Design Decision Matrix

Parameters	Weight	Upright	Reclined	Prone
Rider Comfort	20%	4	4	2
Weight	25%	3	3	4
Aerodynamics	30%	3	3	4
Power Output	25%	5	4	4
Total	100%	3.7	3.45	3.6

Appendix A-3: Fairing Material Design Matrix

Parameters	Weight	Carbon Fiber	Fiberglass	Polycarbonate	Coroplast
Stiffness	35%	5	5	2	4
Manufacturability	20%	2	3	4	3
Cost	20%	2	3	5	5
Weight	25%	5	2	3	2
Total	100%	3.8	3.45	3.25	3.5

Appendix A-4: Seat Design Matrix

Parameters	Weight	Off the Shelf Seat	Custom Made Seat	1/4 Inch Rope Seat	Contoured Seat
Ergonomics	25%	1	4	2	3
Cost	20%	2	1	4	3
Adaptability	15%	1	2	4	3
Weight	10%	1	2	3	4
Aesthetics	15%	2	3	1	4
Attachment	5%	1	4	3	2
Reusable	10%	2	1	4	3
Total	100%	1.45	2.45	2.9	3.2

Appendix A-5: Steering Decision Matrix

Parameters	Weight	Bell Crank Steering	Rack and Pinion Steering	Tractor Steering	Swing Steering
Ergonomics	10%	4	4	2	1
Cost	15%	2	1	4	3
Weight	35%	2	1	4	4
Aesthetics	15%	3	3	2	1
Attachment	25%	4	4	2	2
Total	100%	3.0	2.35	2.65	2.6

Appendix A-6: Suspension Design Matrix

Parameters	Weight	4-Bar Linkage	Normal Spring	Air Spring	Box Design
Adjustability	30%	4	2	2	3
Frame Alterations	30%	3	2	2	1
Weight	20%	4	5	5	1
Manufacturability	15%	2	4	3	1
Aesthetics	5%	4	3	3	3
Total	100%	3.4	2.95	2.8	1.7

Appendix A-7: Carbon Fiber Layup Method

Parameters	Weight	Hand Layup	Resin Infusion	Lamination	Prepreg
Cost	30%	3	3	3	1
Strength	20%	3	3	4	4
Complexity	25%	4	2	3	4
Manufacturability	25%	3	2	4	4
Total	100%	3.25	2.5	3.45	3.1

Appendix B: Material Selection Data

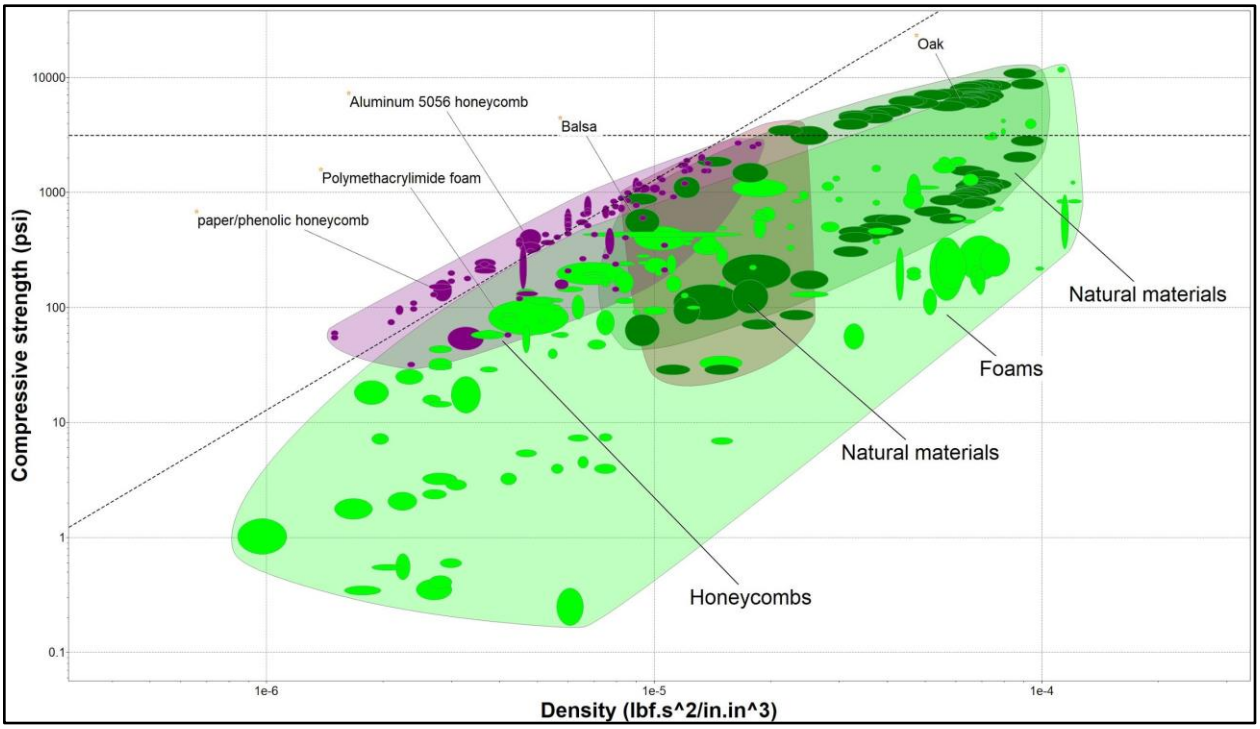

Appendix C: Bottom Bracket (BB) Sandwich Panel Core Layout

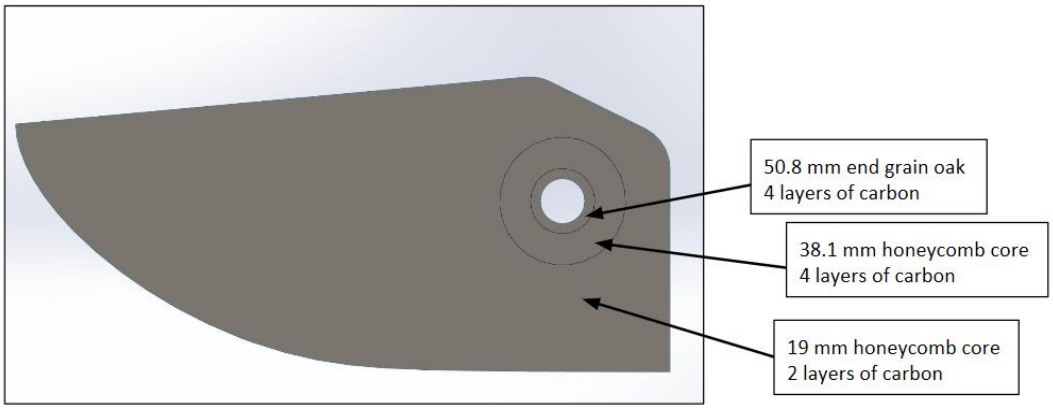

Appendix D: NACA Duct

Appendix D-1: NACA Duct Model

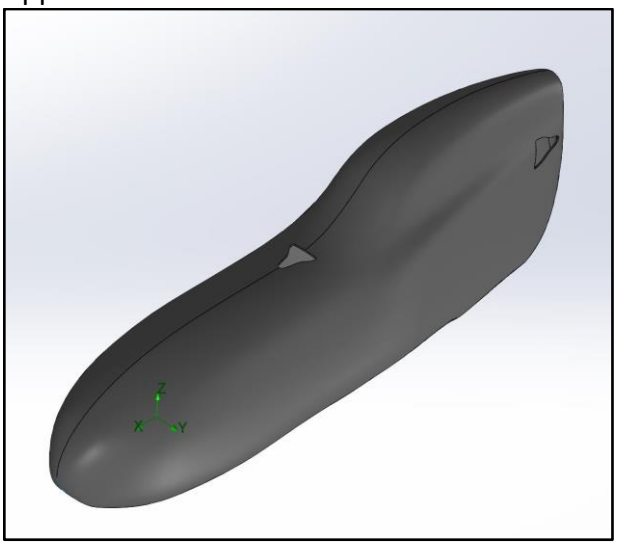

Appendix D-2: NACA Duct Flow Trajectory

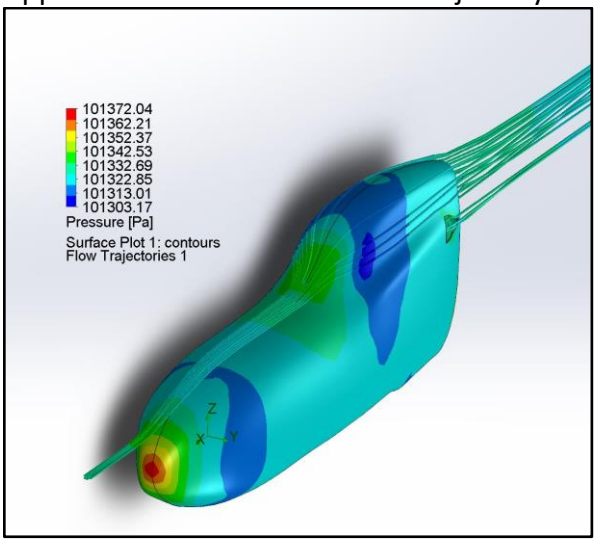

Appendix E: MATLAB Code for Ackerman Angle Calculation

```
%% This Code Creates a Figure that Displays Suitable Independant Turn
%  Angles based on Ackerman's Formula
%
%  Written By: Zack Broadbent
%
%  Nomenclature:
%  1) alpha_i = inner tire turn angle (deg)
%  2) alpha_o = outer tire turn angle (deg)
%  3) L       = Distance between front and rear tires (in)
%  4) R       = Track Radius (ft)
%  5) T       = Distance between kingpin axes (in)
%  6) theta   = neutral steer angle(deg)
%  Example:
%  L = 43.50;
%  T = 26.0;
%  R = 0:1:80;
%  theta =
%
%    65.8545
function [theta] = Ackerman_Compensation(L,T,R)
%% Unit Adjustment (in -> ft)
T       = T/12;
L       = L/12;
%% Calculate Turn Angles/Neutral Steer Angle
alpha_i = atan2(L ,(R-(T/2)));
alpha_o = atan2(L ,(R+(T/2)));
alpha_i = rad2deg(alpha_i);
alpha_o = rad2deg(alpha_o);
theta   = atan2(4*L,3*T);
theta   = rad2deg(theta);
%% Plot Results
figure; plot(R,alpha_i,'g',R,alpha_o,'b')
title('Ackerman"s Compensation')
ylabel('Turn Angle')
xlabel('Track Radius')
figure; plot(alpha_i,alpha_o)
title('Simple Vs. Ideal Steering')
ylabel('Outer Turn Angle')
xlabel('Inner Turn Angle')
```

Appendix F: Rider Dimensions and Summery

Measurement	Jordan	Leland	Marlee	Tia	Duncan	Average	95% Conf. Max.	95% Conf. Min.
Total Height	70.00	69.75	63.00	67.75	74.00	**68.90**	**72.04**	**65.76**
Leg length	36.75	38.00	32.00	37.00	41.00	**36.95**	**39.79**	**34.11**
Top of Knee to Bottom of Foot	21.50	21.00	19.00	23.25	24.00	**21.75**	**23.48**	**20.02**
Torso Length	25.00	25.25	21.00	24.00	24.50	**23.95**	**25.46**	**22.44**
Lower Back Length	11.00	10.00	6.50	8.50	9.50	**9.10**	**10.60**	**7.60**
X-Seam	41.00	41.50	39.75	42.00	45.50	**41.95**	**43.83**	**40.07**
Heel to Toe Length	9.50	9.00	9.00	9.75	10.50	**9.55**	**10.10**	**9.01**
Shoulder Width	18.50	18.00	16.75	18.25	19.25	**18.15**	**18.95**	**17.35**
Shoulder Width	7.25	7.25	6.25	7.00	7.50	**7.20**	**7.77**	**6.63**
Hip Width	15.00	15.00	16.00	14.75	14.00	**14.75**	**15.48**	**14.02**
Arm Length	30.00	30.00	28.00	29.50	33.00	**30.35**	**32.00**	**28.70**

Appendix G: Rider Configuration Test Information

Appendix G-1: Test Configuration Angles

Test	Hip Orientation Angle, HOA	Back Angle, BA	Body Configuration Angle, BCA
1	15°	42°	123°
2	8°	30°	142°
3	8°	42°	130°
4	0°	30°	150°
5	0°	42°	138°
6	0°	57°	123°

Appendix G-2: Depiction of Back Angle, BA, Hip Orientation Angle, HOA, and Body Configuration Angle, BCA

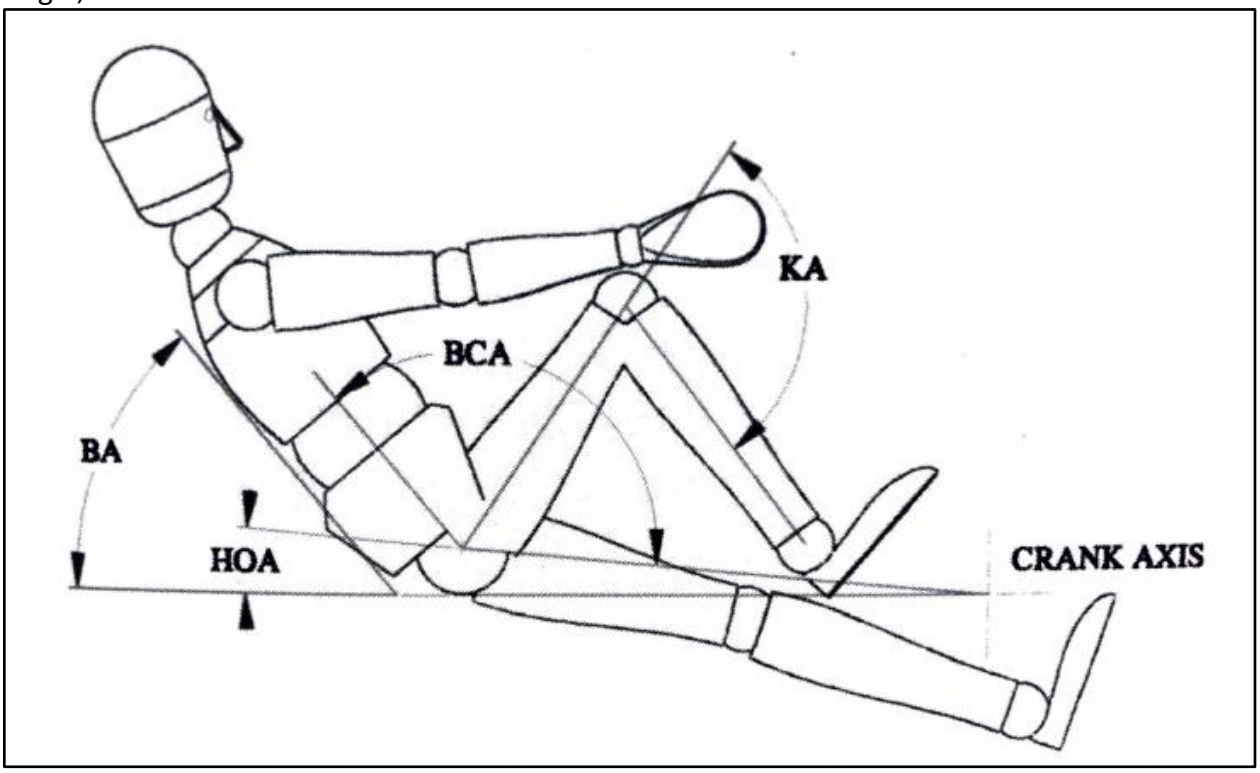

Appendix G-3: Average Power Output in Watts

Test	Leland	Tia	Jordan
1	84	95	100
2	90	90	88
3	94	104	98
4	108	99	95
5	111	98	95
6	104	102	92

Appendix G-4: Graph of Power Output vs Heart Rate